EJMI

DOI: 10.14744/ejmi.2022.11286
EJMI 2022;6(4):387–393

Research Article

The Role of Simultaneous Standardized Uptake Value and MRI Diffusion Weighted Heterogeneity Index from Hybrid PET/MR in the Evaluation of Brain Metastases

Bahattin Ozkul,[1] Bedriye Koyuncu Sokmen,[2] Ibrahim Halil Sever,[2] Ozlem Ozkul,[3] Nagihan Inan Gurcan[2]

[1]Department of Radiology, Istanbul Atlas University Medicine Hospital, Istanbul, Türkiye
[2]Department of Radiology, Demiroğlu Bilim University Florence Nightingale Hospital, Istanbul, Türkiye
[3]Department of Medical Oncology, Medicalpark Florya Hospital, Istanbul, Türkiye

Abstract

Objectives: To evaluate diagnostic performance of apparent diffusion coefficient (ADC) heterogeneity index to differentiate brain metastasis (BM) from normal appearing brain parenchyma (NABP) and to find out the correlation between 2-[^{18}F]-fluoro-2-deoxy-D-glucose (^{18}F-FDG) standardized uptake value (SUV) and ADC heterogeneity index derived from hybrid PET/MRI.

Methods: Brain sequences, which were dixon and diffusion weighted imaging (DWI) protocols with simultaneous PET were used to calculate coefficient of variance of the ADC (ADC_{CV}) and SUV_{max}. Inter-rater reliability was tested by interclass correlation (ICC). The correlation of ADC_{CV} and SUV_{max} and the differences in ADC values, SUV_{max} and combination of ADC values and SUV_{max} between BM and NABP were investigated.

Results: The excellent consistency was found between raters at ADC_{mean} (0.972) and ADCCV (0.995). There was a moderate correlation between ADC_{CV} and SUV_{max} (r=0.585) and a slight inverse correlation between ADC_{mean} and SUV_{max} (r=-0.154). A statistically significant difference between BM and NABP was determined for ADCCV (p<0.001) and SUV_{max} (p<0.001). An area under the curve (AUC) of 0.663, 0.966, 0.571, 0.696 and 0.971were obtained with ROC analysis of SUV_{max}, ADC_{CV}, ADC_{mean}, ADC_{mean}+SUV_{max} and ADC_{CV}+SUV_{max} respectively.

Conclusion: ADC_{CV} may be considered as a potential biomarker that quantitatively discriminates BM from NABP with excellent interrater reliability.

Keywords: ADC_{CV}, brain metastasis, PET/MRI

Cite This Article: *Ozkul B, Koyuncu Sokmen B, Sever IH, Ozkul O, Gurcan NI. The Role of Simultaneous Standardized Uptake Value and MRI Diffusion Weighted Heterogeneity Index from Hybrid PET/MR in the Evaluation of Brain Metastases. EJMI 2022;6(4):387–393.*

Brain metastasis (BM) is associated with poor survival outcomes and poses distinct clinical challenges. Lung cancer, renal cell carcinoma, breast cancer, melanoma and colorectal cancers are the most common causes of BM.[1] Due to great variation in imaging appearances, these metastases present a common diagnostic challenge which can affect patient management.

Computed tomography (CT) and magnetic resonance imaging (MRI) are the key imaging modalities used in the diagnosis of BM. In some cases, advanced imaging techniques including proton magnetic resonance spectroscopy (MRS), contrast enhanced magnetic resonance perfusion (MRP), diffusion weighted imaging (DWI), and diffusion tensor imaging (DTI) may help for the diagnosis.[2] Although these

Address for correspondence: Bahattin Ozkul, MD. Istanbul Atlas Universitesi Tip Hastanesi Radyoloji Anabilim Dali, Istanbul, Türkiye
Phone: +90 532 223 94 63 **E-mail:** bahozkul@yahoo.com

Submitted Date: January 09, 2022 **Accepted Date:** July 16, 2022 **Available Online Date:** September 30, 2022

imaging techniques are essential in the diagnosis, using quantitative data may lead to improved detection of BM.

DWI is a fast, non-contrast MR technique that indicates the random microscopic motion of free water molecules. It is widely appreciated as a qualitative tool in the examination of the central nervous system (CNS). Apparent diffusion coefficient (ADC) is a measure, calculated using DWI and reflects the magnitude of diffusion quantitatively.

Tumors are heterogeneous because of the spatial variation in the cellularity, angiogenesis, extracellular matrix and necrosis.[3, 4] Higher intratumoral heterogeneity is related with poor prognosis due to its aggressive behavior.[5-7] Thus, measuring of tissue heterogeneity may be helpful in the detection of tumors and selection poor prognostic patients for more intensive therapy. There are various methods using complex textural analysis in the detection of tissue heterogeneity.[8] Of all these, the coefficient of variation (CV) is easily calculated and shows relative variability. In line with this, ADC_{CV} as a reliable heterogeneity index was used in different studies.[9-12]

Positron Emission Tomography (PET)/MRI is a new imaging technology that allows for PET and MRI scans to be acquired simultaneously. Although MRI is the standard neuroimaging technique for detection of tumors and the surrounding anatomical structures in the brain, PET aids to complement MRI in lesion grading, tumor extent delineation and evaluation of the treatment response. Allowing both structural and functional evaluation of tumors in one single scan makes PET/MRI more popular in oncology imaging.

The primary target of our study was to determine the diagnostic performance of ADC_{CV}, as a heterogeneity index, to differentiate BM from normal appearing brain parenchyma (NABP), as compared to conventional MRI metrics used in daily routine. A secondary target of this research was to evaluate the efficiency of ADC_{CV} to differentiate BM from NABP when we combined with standard uptake value (SUV_{max}) simultaneous derived from PET-MRI. To the best of our knowledge, this is the first study that evaluates the diagnostic performance of ADC_{CV} in brain metastases and its correlation with SUV_{max} on PET/MRI hybrid system.

Methods

Study Design

347 consecutive adult patients with known malignancies who underwent PET/MRI between January 2017 and September 2019 were evaluated. Forty-five patients who had BM were enrolled in this retrospective single center study. The patients who has multiple lesions (if there is no enough NABP), a massive brain edema and a history of radiotherapy were excluded from the study. Decision of BM was given if lesions growth at least two imaging methods in the follow-up imaging (3-6 months) or proven with biopsy (single lesion). Thus, 49 lesions of 26 patients were included and analyzed for this study (Fig. 1). All primary malignancies were proven histopathological by biopsy or surgery.

Image acquisition

Patients fasted at least 6 hours before starting examination and injection of ^{18}F-FDG was given if blood glucose levels were < 140 mg/dL (7.77 mmol/L). All scans were performed with the patient in the supine position on the 3 Tesla Biograph mMR scanner (Siemens Healthcare, Erlangen, Germany) using a 16-channel head and neck surface coil and three 12-channel body coils and the total scanning time was 60±3 minutes. The whole-body images, which cover the entire body from head to heel, were obtained in five to six bed positions according to body-mass index (BMI) of patient. PET attenuation correction was performed using

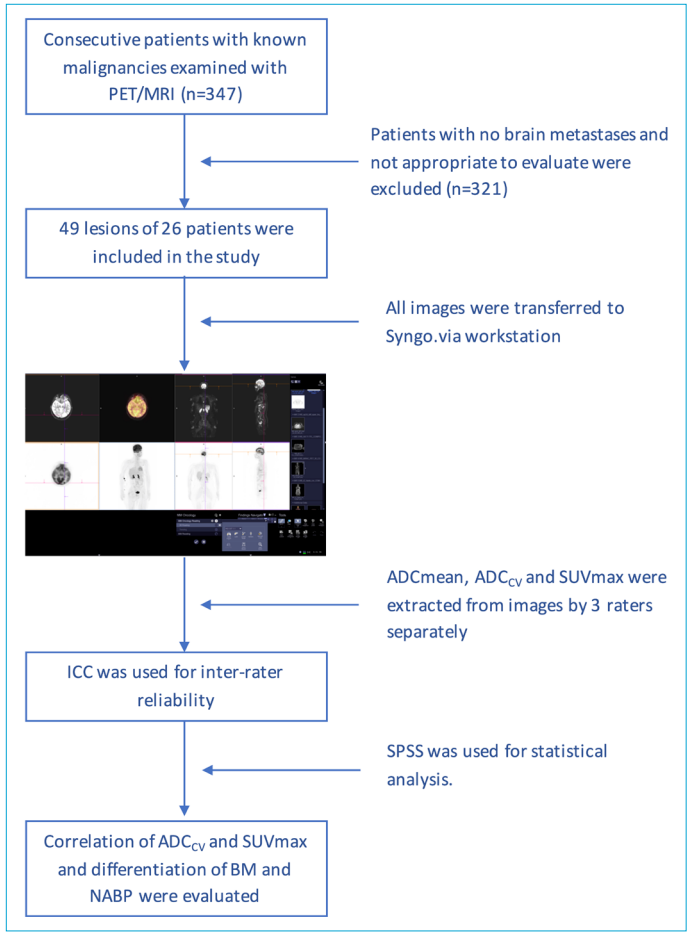

Figure 1. Design of the study.

*ADC: Apparent diffusion coefficient; CV: coefficient of variation; SUV: Standardized uptake value; ICC: Inter-class correlation coefficient; SPSS: Statistical package for the social sciences; BM: Brain metastases; NABP: Normal appearing brain parenchyma.

four compartment model attenuation map calculated from a Dixon-based volumetric interpolated breath-hold examination (VIBE) sequence. The MRI protocol included sequences as below: T1-weighted slice-selective Turbo Flash (TR/TE, 1600 msec / 2.5 msec) in the axial plane, free breath diffusion-weighted imaging using the echo planar imaging technique (EPI) (TR/TE, 12000 msec / 78 msec, b=0 s/mm^2 and 800 s/mm^2) in the axial plane and T2-weighted single-shot echo train (HASTE) (TR/TE, 1500 msec / 87 msec) in the coronal plane. Contrast enhanced protocol including the breath-hold 3D VIBE sequence (TR/TE, 4.56 msec / 2.03 msec) in the arterial, portal venous and equilibrium phases covering whole-body in the axial plane was performed with using a weight-adapted gadolinium-based contrast agent and all sections were then combined.

Image Analysis

All image datasets were transferred to the dedicated Syngo.via PET/MRI workstation (Siemens Healthcare) and images were assessed separately by three radiologists (İ.H.S, B.K.S and N.İ.G) with at least 7 years of experience who were blinded to the patients' information. A volume of interest (VOI) was placed manually on axial PET images and all three planes were controlled for ensuring to not overflow the limits of the lesions. The VOI was coregistered and placed on ADC images overlapping with PET images. Manual correction was used to fine tune when the images were not overlapped. For each determined lesion, a similar size of VOI was used on NABP (Fig. 2). Care was taken to keep away from edema, blood vessels and cerebrospinal fluid and for preventing bias, white matter, which did not include sulcus, was used to evaluate NABP. SUV_{max}(SUV of the hottest voxel within a defined VOI), which is easy to use and operator independent, was calculated automatically and measured on PET images. The mean (ADC_{mean}) and standard deviation (SD) of ADC (ADC_{SD}) were calculated automatically by software for each measurement. ADC_{CV} was created by dividing the SD by the ADC_{mean}.

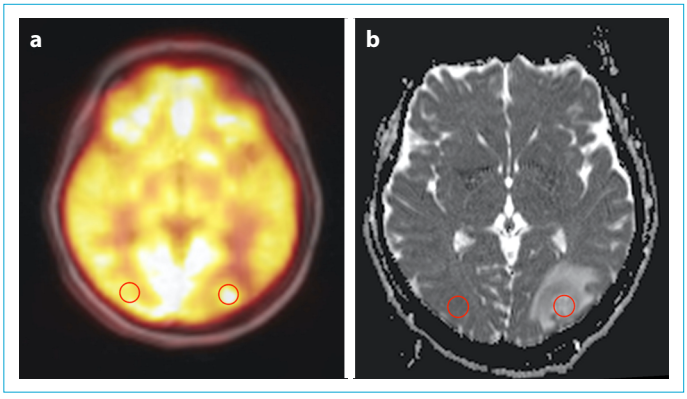

Figure 2. Replacing the VOI **(a)** Two VOIs with same size was drawn on brain metastasis and normal appearing brain parenchyma with giving care to tumor margins on axial SUV-PET images **(b)** Both VOI was copied and placed with the same location on axial ADC images.

Statistical Analysis

IBM Statistical Package for the Social Sciences (SPSS ver. 21 for windows, Chicago, IL, USA) software was used for all statistical analysis. Intra-class correlation coefficient (ICC) was used for determining inter-rater reliability in variables. The ICC value " <0.50, 0.51-0.75, 0.76-0.90 and > 0.90 were evaluated as indicating poor, moderate, good and excellent reliability, respectively. The fitness of numeric data set to normal distribution was determined by the Shapiro-Wilk test. Due to normal distribution, correlation between $SUV_{max}$and ADC_{CV} was tested by Pearson correlation. Independent t test was carried out to measure differences between BM and NABP for all variables. Receiver operating characteristics (ROC) analysis based on histopathological results was performed to determine cut-off value, which differentiate BM from NABP, by the Youden index. The area under the curve (AUC), sensitivity and specificity were calculated for each variable. A p-value 0.05 was accepted as statistically significant.

Results

Patients Demographic

Twenty-six patients (15 female, 11 male) with proven BM were included in the study. The patients aged between 28-87 (mean±standard deviation; 63.7±16.4) years. 20 patients (77%) also had metastases in other locations besides the brain. 49 BM were analyzed with VOI mean mean 3.57±2.13 cm^3. As identified in table 1, breast (invasive ductal carcinoma, 5 patients; invasive lobular carcinoma, 4 patients), lung (adenocarcinoma, 7 patients; small cell carcinoma, 3 patients), colon (adenocarcinoma, 4 patients), kidney (renal cell carcinoma, 2 patients) and skin (malignant melanoma, one patient) were the primary source of tumors for BM.

Interrater Reliability

There was an excellent consistency between raters at ADC_{mean}, ADC_{SD}, ADC_{CV} and $SUV_{max}$with ICC 0.972 [95% confidence interval (CI] 0.952-0.984), 0.990 (95% CI 0.983-0.994), 0.995 (95% CI 0.992-0.997) and 0.993 (95% CI 0.989-0.996), respectively.

Correlation with SUV_{max}

For all values, the mean of three raters was calculated and presented as ADC_{mean}, ADC_{CV} and SUV_{max}. According to Pearson correlation coefficient, there was a moderate positive correlation (r=0.585, p<0.000) between ADC_{CV} and SUV_{max}

Table 1. Primary source and histopathology of metastases and distribution of the study population

Primary Source	Histopathology	No. of patients	No. of metastases
Breast	Invasive ductal	5	11
	Invasive lobular	4	9
Lung	Adenocarcinoma	7	9
	Small cell carcinoma	3	5
Colon	Adenocarcinoma	4	6
Kidney	Renal cell carcinoma	2	3
Skin	Malignant melanoma	1	6
Total		26	49

when all measurements included (BM+NABP). A negligible inverse correlation was found between ADC_{mean} and SUV_{max} (r=-0.154, p=0.044).

Differences between BM and NABP

A statistically significant difference between BM and NABP with p<0.001 and =0.007 value was found for ADC_{CV} and SUV_{max}, respectively. There was no statistically significant difference for ADC_{mean} (p=0.076). The mean±SD values of ADC_{mean}, ADC_{CV} and SUV_{max} of all lesions were presented in the table (Table 2).

The cut-off value based on the maximum Youden index to determine differentiation between BM and NABP was ≥3.34 for SUV_{max}, 0.84 x10^{-3} mm^2/s for ADC_{mean} and ≥0.08 for ADC_{CV}. An AUC for SUV_{max} of 0.663 (95% CI 0.544-0.782, p=0.012) was yielded with ROC curve analysis. ADC_{CV} (AUC:0.966, p<0.001) had higher AUC with a smaller standard error and a narrower confidence interval than ADC_{mean} (AUC: 0.571, p=0.273) and SUV_{max} (Fig. 3). The sensitivity and specificity of ADC_{CV} (82.5%, 97.5%, respectively) were higher than SUV_{max} (67.5%, 60%, respectively) and ADC_{mean} (55%, 70%, respectively). When we combined SUV_{max} and ADC_{mean} to discriminate BM and NABP, the AUC was 0.696 (95% CI 0.581-0.810) yielding a better sensitivity (70%). The highest AUC (0.971) was found in combination of ADC_{CV} and SUV_{max} with a sensitivity of 97.5% and specificity of 87.5% (Fig. 4). AUC, sensitivity, specificity, confidence interval and standard error of all values were summarized in the table (Table 3).

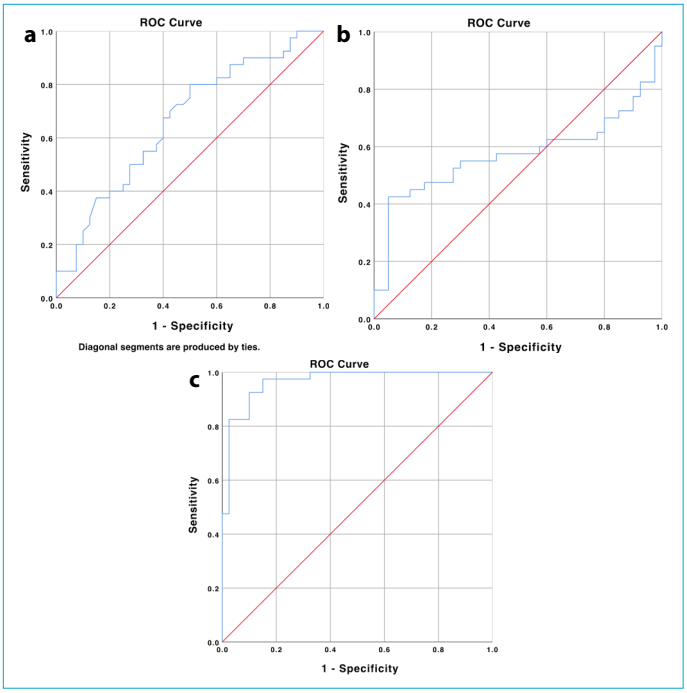

Figure 3. Receiver operating characteristics (ROC) curve and area under the curve (AUC) of **(a)** SUV_{max}, **(b)** ADC_{mean} and **(c)** ADC_{CV} to discriminate brain metastasis and normal appearing brain parenchyma.

Discussion

In this study, we investigated the role of ADC_{CV} derived from PET/MRI as a heterogeneity index in discriminating BM from NABP. The main finding of this study was that, ADC_{CV} is more effective to discriminate BM from NABP compared to conventional ADC parameters. Besides, ADC_{CV} had

Table 2. A comparison between SUV and ADC data according to mean of three raters in normal appearing brain parenchyma and brain metastases

Variable (n=49)	Normal appearing brain parenchyma†	Brain metastases†	p-two tailed‡
SUV_{max}	3.19±0.55	3.51±0.49	0.007
ADC_{mean} (10-3 mm^2/s)	0.82±0.07	0.86±0.15	0.076
ADC_{CV}	0.05±0.02	0.11±0.03	<0.001

*SUV: Standardized uptake value; ADC: apparent diffusion coefficient; CV: coefficient of variance; †mean±Standard deviation; ‡Independent t test.

Table 3. Receiver operating characteristics analysis

Variable	AUC	SE	95% Confidence interval	Sensitivity (%)	Specificity (%)	p
SUV_{max}	0.663	0.061	0.544-0.782	67.5	60	.012
ADC_{mean}	0.571	0.069	0.436-0.706	55	70	.273
ADC_{CV}	0.966	0.018	0.931-1.000	82.5	97.5	<.001
SUV_{max} + ADC_{mean}	0.696	0.058	0.581-0.810	70	65	.003
SUV_{max} + ADC_{CV}	0.971	0.016	0.940-1.000	97.5	87.5	<.001

*AUC: Area under the curve; SE: Standard error; SUV: Standardized uptake value; ADC: Apparent diffusion coefficient; CV: Coefficient of variance.

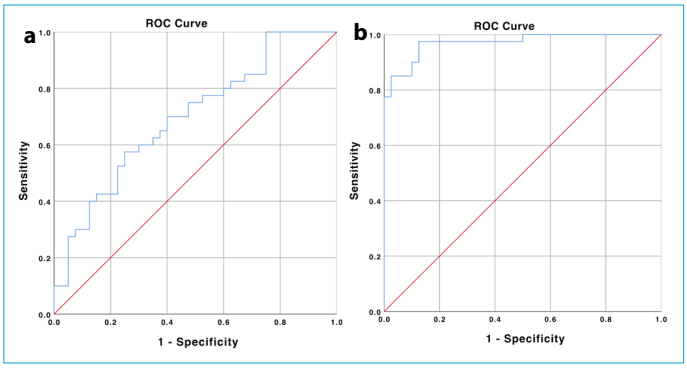

Figure 4. Receiver operating characteristics (ROC) curve and area under the curve (AUC) of **(a)** SUV_{max} + ADCmean, **(b)** SUV_{max} + ADC_{cv} to discriminate brain metastasis and normal appearing brain parenchyma.

higher potential to discriminate BM from NABP when we combined with SUV_{max} from simultaneous derived PET/MRI system.

Integrated PET/MRI scanners with the recent developments, new opportunities have emerged for quantitative molecular imaging. PET / MRI provides multimodal analysis of concurrently acquired functional parameters that can contribute to better characterization of tumor biology and also help identify markers to predict response to therapy.[13, 14]

Due to the high ^{18}F-FDG uptake of the cerebral cortex and the low spatial resolution of PET imaging, FDG PET/CT imaging has limitations, especially in the detection of small metastases in the brain. Sensitivity of FDG PET/CT in brain imaging is low. In retrospective comparative studies, it is stated that FDG PET/CT imaging at the time of diagnosis can capture up to 61% of metastatic brain lesions that can be detected by MRI.[15] Therefore, PET / MR imaging may be preferred in brain metastasis scanning because of the high soft tissue contrast of MR imaging.

SUV_{max} measured by PET and ADC measured by MRI allow assessment of water diffusion and glucose metabolism in tumor cells. The results of the present study show that ADC_{CV} exhibits an improved correlation with SUV_{max}. Moreover, it provides better quantitative separation between BM and NABP, as compared to common MRI metrics.

In this study, ADC_{mean} showed a significant negative correlation with SUV_{max}; however, ADC_{CV} showed higher correlation with SUV_{max} than ADC_{mean} parameter. There are previously reported oncologic studies of the inverse correlation found between ADC and SUV. Several of these studies reported significant strong inverse correlation between ADC_{mean} and SUVpeak in rectal cancer,[16] a significant inverse correlation between ADC_{mean} and SUVmean in gastrointestinal stromal tumor,[17] and recently an inverse correlation between ADC and PET SUV in liver tumors.[18]

Tumor heterogeneity consists of marked differences in cell mix, size, and arrangement. Heterogeneity also plays a role in micro-environmental factors (including oxygenation, pH, interstitial pressure, blood flow), metabolism, and gene expression. This deep heterogeneity is extremely important for prognosis, treatment planning, and drug distribution, which ultimately affects patient outcomes. There are a number of ways to investigate tumor heterogeneity, some of which include functional and molecular imaging, which can be applied to clinical data.[19]

The characterization of tissues can be improved using histogram-based assessments of the distribution of ADC values. Histogram approaches have multiple advantages, including volume-of-interest (VOI) assessments, thus avoiding the subjectivity that is inherent with ROI placements. Importantly, histograms can provide additional metrics that reflect the texture of lesions, thereby allowing heterogeneity of ADC distribution within tissue to be assessed.[20] Tissue heterogeneity analysis is rapidly evolving by various methods. Despite most of the tools currently offered are often complex and computationally costly, it is an easy to calculate texture parameter of ADC_{CV}. Several studies have used CV as an index of heterogeneity in recent years.

In a study in liver metastasis, the results of this study show that ADC_{CV} can significantly distinguish between liver metastasis and normal-appearing liver.[9] Similar to our study, there was a good correlation between ADC_{CV} and SUV peak in this study. Significant differences in CV diffusion index was found in another study about hepatocellular carcinoma in fresh liver explants.[21]

PET/CT and DWI share applications in clinical oncology. While both SUV and ADC correlate with cellularity, SUV is also associated with several other pathological markers such as mitotic count, presence or absence of necrosis. [22] For this reason, PET/MRI oncological evaluation is also valuable when these two parameters (SUV and ADC) are obtained together in the same examination. In a study by Nakajo et al.,[23] 44 patients with breast cancer underwent preoperative PET/CT and DWI within an average of 17 days between examinations, and both SUV_{max} and ADC were significantly associated ($p<0.05$) with histologic grade (independently), nodal status, and vascular invasion. This finding suggests that SUV_{max} and ADC correlate with several of the pathologic prognostic factors and that both values may have the same potential for being predictive of the prognosis of breast cancer.

In oncology, imaging has a very important place in evaluating response to treatment. For this reason, many studies are aimed at understanding the structure and heterogeneity of the tumor. Therefore, it is essential to develop quantitative imaging methods and objective biomarkers to improve the diagnosis of brain metastasis. As a volume-independent index of heterogeneity, ADC_{CV} can be considered as a potential biomarker that quantitatively differentiates BM from NABP. Tissue heterogeneity has been proposed as a basis for a biomarker for tumors.[3, 4, 24]

This hybrid PET/MRI study shows a significant negative correlation between metabolic activity on ^{18}F-FDG PET and water diffusion over DWI in brain metastasis, possibly because both parameters are directly related to tumor cellularity. The correlation found between SUVs and ADC_{mean}, ADC_{CV} values supports the idea that high cellularity due to tumor proliferation results in greater metabolic activity and restricts water diffusion.

Nowadays, using multi-parametric brain MRI (MR spectroscopy, MR perfusion, DWI, routine contrast enhanced MRI) to evaluate cranial pathologies becomes a routine practice. We think that ADC_{CV} has a potential to evaluate tumor heterogeneity and may be a new parameter in multi-parametric MRI. Studies on differentiating local recurrence in brain tumor and radiotherapy associated changes or tumor and other cranial pathologies (brain abscess, leukodsytrophy, lymphoma, etc) may support our hypothesis.

This study has several limitations. First, this was a retrospective study and performed on a relatively small study population. Another limitation was the difficulty in determining the limits of the lesions due to the limited resolution of PET. The accuracy of the results obtained from our study should be supported by using different software in larger patient groups and with multi-center studies. The last limitation of our study was that brain metastases originated from different sources.

Conclusion

In conclusion, using PET/MRI instead of PET/CT decreases radiation dose, however radiation exposure caused by short term follow-up imaging of oncology patients continue to be an issue. Although determining brain metastases compared to normal brain parenchyma are not the main challenge in oncologic patients, ADC_{CV} may be helpful to clinicians for avoiding further radiation exposure of patients and for managing patients when using contrast media is contraindicated. Moreover, it would be easy to implement ADC_{CV} in a clinical setting. Future studies that will blindly and independently identify BM in NABP using PET ^{18}F-FDG SUV and DWI ADC_{CV} will present potential to investigate ADC_{CV} as a new parameter for BM.

Disclosures

Ethics Committee Approval: This study was performed in line with the principles of the Declaration of Helsinki. Approval was granted by the Ethics Committee of Demiroğlu Bilim University (Date. 27.10.2020/No. 2020-20-04).

Peer-review: Externally peer-reviewed.

Funding: This research did not receive any specific grant from funding agencies in the public, commercial, or not-for-profit sectors.

Conflict of interest: The authors have no relevant financial or non-financial interests to disclose.

Consent to participate: Informed consent was obtained from all individual participants included in the study.

Consent for publication: Patients signed informed consent regarding publishing their data.

Availability of data and material: The datasets analyzed in the current study are available from the corresponding author on reasonable request.

Code availability: Syngo.via (Material no: 10496180, Serial no: 130408) IBM SPSS V.21 (Authorization code: 4b37d8fed81bc545db11).

Acknowledgement: Partial part of our manuscript has been presented as an oral presentation in the Congress of Turkish Society of Neuroradiology 2020, Istanbul.

Authorship Contributions: Concept – B.O.; Design – B.O.; Supervision – N.İ.G; Materials – I.H.S., B.K.S.; Data collection and processing – B.O., B.K.S.; Analysis and interpretation – B.K.S., I.H.S, N.I.G; Literature search – B.O., B.K.S., I.H.S.; Writing – B.O., B.K.S., I.H.S.; Critical review – O.O.

References

1. Kumar V, Abbas AK, Fausto N, Robbins SL. Robbins and Cotran pathologic basis of disease. Elsevier Saunders; 2005.

2. Fink KR, Fink JR. Imaging of brain metastases. Surg Neurol Int 2013;4:S209–19. [CrossRef]
3. Boroughs LK, DeBerardinis RJ. Metabolic pathways promoting cancer cell survival and growth. Nat Cell Biol 2015;17:351–9.
4. Robertson-Tessi M, Gillies RJ, Gatenby RA, Anderson AR. Impact of metabolic heterogeneity on tumor growth, invasion, and treatment outcomes. Cancer Res 2015;75:1567–79.
5. Ganeshan B, Miles KA, Young RC, Chatwin CR. Hepatic entropy and uniformity: additional parameters that can potentially increase the effectiveness of contrast enhancement during abdominal CT. Clin Radiol 2007;62:761–8. [CrossRef]
6. Ganeshan B, Abaleke S, Young RC, Chatwin CR, Miles KA. Texture analysis of non-small cell lung cancer on unenhanced computed tomography: initial evidence for a relationship with tumour glucose metabolism and stage. Cancer Imaging 2010;10:137–43. [CrossRef]
7. Miles KA, Ganeshan B, Griffiths MR, Young RC, Chatwin CR. Colorectal cancer: texture analysis of portal phase hepatic CT images as a potential marker of survival. Radiology 2009;250:444–52. [CrossRef]
8. Alic L, Niessen WJ, Veenland JF. Quantification of heterogeneity as a biomarker in tumor imaging: a systematic review. PLoS One 2014;9:e110300. [CrossRef]
9. Stein D, Goldberg N, Domachevsky L, Bernstine H, Nidam M, Abadi-Korek I, et al. Quantitative biomarkers for liver metastases: comparison of MRI diffusion-weighted imaging heterogeneity index and fluorine-18-fluoro-deoxyglucose standardised uptake value in hybrid PET/MR. Clin Radiol 2018;73:832.e17–e22. [CrossRef]
10. Dong X, Wu P, Sun X, Li W, Wan H, Yu J, et al. Intra-tumour 18F-FDG uptake heterogeneity decreases the reliability on target volume definition with positron emission tomography/computed tomography imaging. J Med Imaging Radiat Oncol 2015;59:338–45. [CrossRef]
11. Yoon HJ, Kim Y, Kim BS. Intratumoral metabolic heterogeneity predicts invasive components in breast ductal carcinoma in situ. Eur Radiol 2015;25:3648–58.
12. Bundschuh RA, Dinges J, Neumann L, Seyfried M, Zsótér N, Papp L, et al. Textural parameters of tumor heterogeneity in ^{18}F-FDG PET/CT for therapy response assessment and prognosis in patients with locally advanced rectal cancer. J Nucl Med 2014;55:891–7. [CrossRef]
13. Yankeelov TE, Peterson TE, Abramson RG, Izquierdo-Garcia D, Arlinghaus LR, Li X, et al. Simultaneous PET-MRI in oncology: a solution looking for a problem? Magn Reson Imaging 2012;30:1342–56.
14. Punwani S, Taylor SA, Saad ZZ, Bainbridge A, Groves A, Daw S, et al. Diffusion-weighted MRI of lymphoma: prognostic utility and implications for PET/MRI? Eur J Nucl Med Mol Imaging 2013;40:373–85.
15. Rohren EM, Provenzale JM, Barboriak DP, Coleman RE. Screening for cerebral metastases with FDG PET in patients undergoing whole-body staging of non-central nervous system malignancy. Radiology 2003;226:181–7. [CrossRef]
16. Wong CS, Gong N, Chu YC, Anthony MP, Chan Q, Lee HF, et al. Correlation of measurements from diffusion weighted MR imaging and FDG PET/CT in GIST patients: ADC versus SUV. European Journal of Radiology 2012;81:2122–6. [CrossRef]
17. van Rijswijk CS, Geirnaerdt MJ, Hogendoorn PC, Peterse JL, van Coevorden F, Taminiau AH, et al. Dynamic contrast-enhanced MR imaging in monitoring response to isolated limb perfusion in high-grade soft tissue sarcoma: initial results. Eur Radiol 2003;13:1849–58. [CrossRef]
18. Kong E, Chun KA, Cho IH. Quantitative assessment of simultaneous F-18 FDG PET/MRI in patients with various types of hepatic tumors: Correlation between glucose metabolism and apparent diffusion coefficient. Plos One 2017;12:e0180184–e.
19. Just N. Improving tumour heterogeneity MRI assessment with histograms. Br J Cancer 2014;111:2205–13. [CrossRef]
20. Dalili D, Padhani A, Grimm R. Quantitative WB-MRI with ADC histogram analysis for response assessment in diffuse bone disease. Magnetom Flash 2017;3.
21. Rosenkrantz AB, Sigmund EE, Winnick A, Niver BE, Spieler B, Morgan GR, et al. Assessment of hepatocellular carcinoma using apparent diffusion coefficient and diffusion kurtosis indices: preliminary experience in fresh liver explants. Magn Reson Imaging 2012;30:1534–40. [CrossRef]
22. Rakheja R, Makis W, Skamene S, Nahal A, Brimo F, Azoulay L, et al. Correlating metabolic activity on 18F-FDG PET/CT with histopathologic characteristics of osseous and soft-tissue sarcomas: a retrospective review of 136 patients. AJR Am J Roentgenol 2012;198:1409–16.
23. Nakajo M, Kajiya Y, Kaneko T, Kaneko Y, Takasaki T, Tani A, et al. FDG PET/CT and diffusion-weighted imaging for breast cancer: prognostic value of maximum standardized uptake values and apparent diffusion coefficient values of the primary lesion. Eur J Nucl Med Mol Imaging 2010;37:2011–20.
24. Marusyk A, Polyak K. Tumor heterogeneity: causes and consequences. Biochim Biophys Acta 2010;1805:105–17.